DOI: 10.5604/01.3001.0013.7944

Volume 97 • Issue 1 • November 2019

Journal of Achievements in Materials and Manufacturing Engineering

International Scientific Journal published monthly by the World Academy of Materials and Manufacturing Engineering

Study of solidification behaviour and mechanical properties of arc stud welded AISI 316L stainless steel

M.H. Abass [a], M.S. Alali [b,*], W.S. Abbas [c], A.A. Shehab [d]

[a] Ministry of Oil, Midland Oil Company, Iraq

[b] Department of Materials Engineering, Faculty of Engineering, University of Kufa, Najaf, Iraq

[c] Babylon Technical Institute, Al-Furat Al-Awsat Technical University, Babylon, Iraq

[d] Department of Materials Engineering, College of Engineering, University of Diyala, Diyala, Iraq

* Corresponding e-mail address: mowahid.alali@uokufa.edu.iq

ABSTRACT

Purpose: This paper aims to investigate the impact of arc stud welding (ASW) process parameters on the microstructure and mechanical properties of AISI 316L stainless steel stud/plate joint.

Design/methodology/approach: The weld performed using ASW machine. The influence of welding current and time on solidification mode and microstructure of the fusion zone (FZ) was investigated using optical microscope and scanning electron microscope (SEM). Microhardness and torque strength tests were utilised to evaluate the mechanical properties of the welding joint.

Findings: The results showed that different solidification modes and microstructure were developed in the FZ. At 400 and 600 A welding currents with 0.2 s welding time, FZ microstructure characterised with single phase austenite or austenite as a primary phase. While with 800 A and 0.2 s, the microstructure consisted of ferrite as a primary phase. Highest hardness and maximum torque strength were recorded with 800 A. Solidification cracking was detected in the FZ at fully austenitic microstructure region.

Research limitations/implications: The main challenge in this work was how to avoid the arc blow phenomenon, which is necessary to generate above 300 A. The formation of arc blow can affect negatively on mechanical and metallurgical properties of the weld.

Practical implications: ASW of austenitic stainless steel are used in multiple industrial sectors such as heat exchangers, boilers, furnace, exhaust of nuclear power plant. Thus, controlling of solidification modes plays an important role in enhancing weld properties.

Originality/value: Study the influence of welding current and time of ASW process on solidification modes, microstructure and mechanical properties of AISI 316 austenitic stainless steel stud/plate joint.

Keywords: Arc stud welding, AISI 316L stainless steel, Solidification mode, Solidification cracking, Second phase

Reference to this paper should be given in the following way:
M.H. Abass, M.S. Alali, W.S. Abbas, A.A. Shehab, Study of solidification behaviour and mechanical properties of arc stud welded AISI 316L stainless steel, Journal of Achievements in Materials and Manufacturing Engineering 97/1 (2019) 5-14.

MATERIALS

1. Introduction

Welding of pins, nuts and bolts that are used in different industrials sectors such as automobiles and structural manufacturing, is very common [1,2]. Conventional arc welding processes such as shielded metal arc welding (SMAW), gas metal arc welding (GMAW) and gas tungsten arc welding (GTAW) are normal candidate for such applications [1]. However, these methods are slow and produce high heat input that can lead to poor productivity and potential defects such as corrosion cracking and heterogeneity of mechanical properties [3,4]. Arc stud welding (ASW) technique offers effective and practical way to replace the conventional welding methods. This technique is originally designed to join a metal stud to a base metal (BM) [5].

ASW process utilises the heat generated by an electric arc to melt a very small area and applies pressure to make the joint [5]. The welding operation consumes very short time (portions of second) to generate the weld [6,7]. This very short time can significantly lower the heat input, minimise the risk of distortion and produce limited fusion zone (FZ) and heat affected zone (HAZ) [8]. However, the microstructure of the FZ especially in austenitic stainless steel is very complicated and sensitive to welding parameters such as welding current and time [9]. Different types of stable and metastable phases of austenite and ferrite can be found in the FZ produced by the phase transformations and solidification behaviour that can be strongly linked to the welding parameters [3]. For instance, the power and speed of the welding process directly affects the solidification mode and dominating phase in the weld microstructure for specific composition. High amount of heat input raises the density of ferrite in the weld metal and increases the dendritic structure size [10-12] .

Another example is given by extremely high speed welding processes such as laser and electron beam welding techniques, which can modify the solidification behaviour in the FZ and promote more austenite over ferrite phase [13-16]. Thus, controlling welding parameters governs the microstructure, which has a great impact on the mechanical properties of the weldment [17,18]. It was reported that presence of ferrite in a particular amounts in the weld metal increases strength of the weldment [12,19]. The existence of the second phase is necessary to prevent the solidification cracking and improve the weldability of the stainless steel by resisting crack propagation [20]. Fine dendrite spacing resulted from low heat input and high welding speed also improves the mechanical properties of the weld metal [10,21]. Therefore, an important attention should always be taken to control the weld microstructure. However, limited literatures have been found deal with the microstructure characterisation of the stainless steel weld made by ASW process [1,2]. Yet, they did not study the effect of welding conditions on solidification behaviour. For this reason, this project aims to understand the solidification modes that exhibited in austenitic stainless steel weld produced by ASW process. The effect of welding parameters on the microstructure and mechanical properties of the joint was investigated throughout the paper.

2. Experimental work

AISI 316L stainless steel was used for both the stud and the BM. The studs were partially threaded with dimensions of M10×70 mm. The BM were plates with dimensions of 70×70×8 mm. The BM were received in as rolled and annealed condition. The chemical composition of stud and plate is listed in Table 1.

The welding operation was performed using ASW machine type DABOTEK DT (1000). Three different welding currents with three welding times were applied in this study, the applied welding parameters are listed in Table 2. A part of welded AISI 316L stainless steel stud to BM sample is shown in Figure 1.

Weld microstructure was examined using optical microscope and scanning electron microscope (SEM) using secondary electron mode. Prior to examination, the weldments were machined then micro-prepared using standard grinding and polishing techniques. To reveal the microstructure, the samples were etched in a solution-mixture consisting of three parts of HCL, two parts of HNO_3 and two parts of acetic acids for 50-60 s. Etching method was according to ASM metal handbook [22].

Table 1.
Chemical composition of AISI 316L BM and stud

Element	C	Si	Mn	Cr	Ni	Mo	Fe
Wt.% BM	0.023	0.570	1.120	17.200	11.400	2.040	Bal.
Wt.% Stud	0.026	0.581	1.130	17.100	11.300	2.030	Bal.

Table 2.
ASW parameters

Sample No.	Welding current, A	Welding time, s
1	400	0.2
2	400	0.3
3	400	0.4
4	600	0.2
5	600	0.3
6	600	0.4
7	800	0.2
8	800	0.3
9	800	0.4

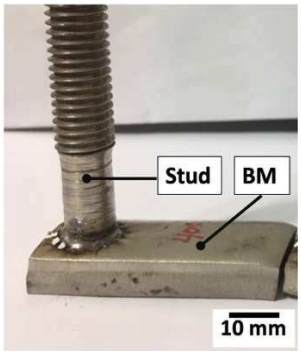

Fig. 1. A part of welded AISI 316L stainless steel stud to BM

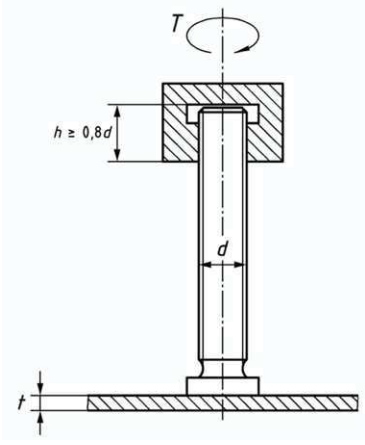

Fig. 2. Torque test assembly according to the BS EN ISO 14555:2014, where T: torque, d: stud diameter, h: length of threaded part of the nut, t: BM plate thickness

Mechanical properties of the weldments were evaluated using microhardness and torque strength tests. Vickers microhardness measurements were implemented along the BM, HAZ and FZ cross section. LARYEE microhardness testing device was used and the measurements were taken using 500 g load and 15 s dwell time. Torque test was performed according to the BS EN ISO 14555:2014 [2] as illustrated in Figure 2.

3. Results and discussion

3.1. Microstructure analysis

The microstructure analysis of three samples welded with three welding currents 400, 600 and 800 A and 0.2 s welding time was carried out. Figure 3 and 4 show the microstructure of different regions in FZ of 400 and 600 A respectively. It can be seen that the solidification mode is full austenitic (A) in both conditions [23]. However, according to the WRC-1992 that introduced by welding research council in 1992 and considered the most reliable constitutional diagram to date [23], the weld metal lies in the ferrite-austenite mode (FA) region as shown in Figure 5. This can lead to an inference that this diagram may not be applicable in this particular condition. It is believed that low welding current and very short welding time caused a diffusionless transformation and growth of austenite as a primary phase instead of ferrite [24]. It can be concluded that the solidification behaviour in welded stainless steel stud is quite similar to that produced with extremely high speed welding processes such as laser and electron beam welding where low heat input and high power density conditions are applied [14,25]. Very low thermal gradient in stud welding process combined with low heat dissipation in stainless steels due to their low thermal conductivity lead to reduce thermal gradient at the weld zone; consequently, columnar and equiaxed solidification modes are preferred to occur instead of planar and cellular.

Austenite structure, Figure 3 and 4, is mainly consisted of columnar dendritic and equiaxed morphologies. Generally, the columnar grains formed in the outer portion

of the FZ and equiaxed located in the central portion. This can be explained in terms of the effect of thermal gradient (G) and growth rate (R). Low G/R ratio at weld centre contributes toward the formation of equiaxed grains structure [7,26].

It is worthy to mention that weld solidification cracking was detected at 600 A 0.2 s as shown in Figure 6. One of the main drawbacks in the full A solidification mode is the high possibility of crack formation during solidification [13,27]. The reason for high cracking susceptibility is single phase microstructure that is straighter than dual phase solidification mode such as austenite-ferrite (AF) and FA as a result of the absence of second phase effect during solidification that resists the crack growth [12,28]. Interestingly, it was observed that the crack was located mostly along the solidification mode transition region, i.e. columnar to equiaxed transition as illustrated in Figure 6. This transition region called 'parting', which considered the weakest part in the microstructure as it showed lowest resistance to shear stresses [3].

It was observed that increasing welding current to 800 A and keeping welding time constant, causes a change in solidification behaviour where FA solidification mode was detected in the microstructure as shown in Figure 7. It is possibly that the higher heat input retards the rapid cooling rate and gives more time for ferrite to exist and solidify as a primary phase [29]. The FA microstructure was free of solidification cracking, this could be related to high crack resistance of the dual phase microstructure [15,30].

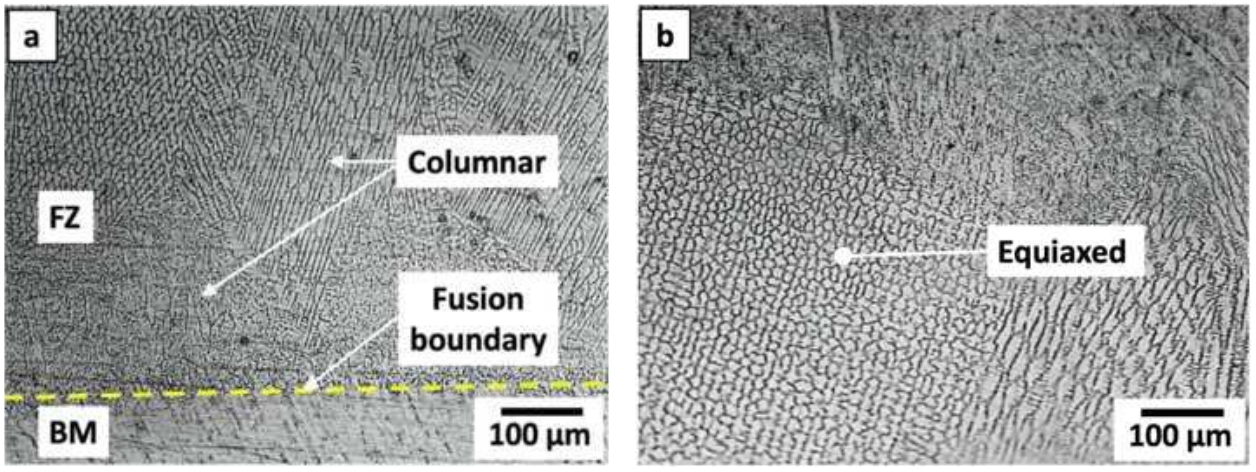

Fig. 3. FZ microstructure of 400 A and 0.2 s at (a) fusion boundary (b) centre of the weld

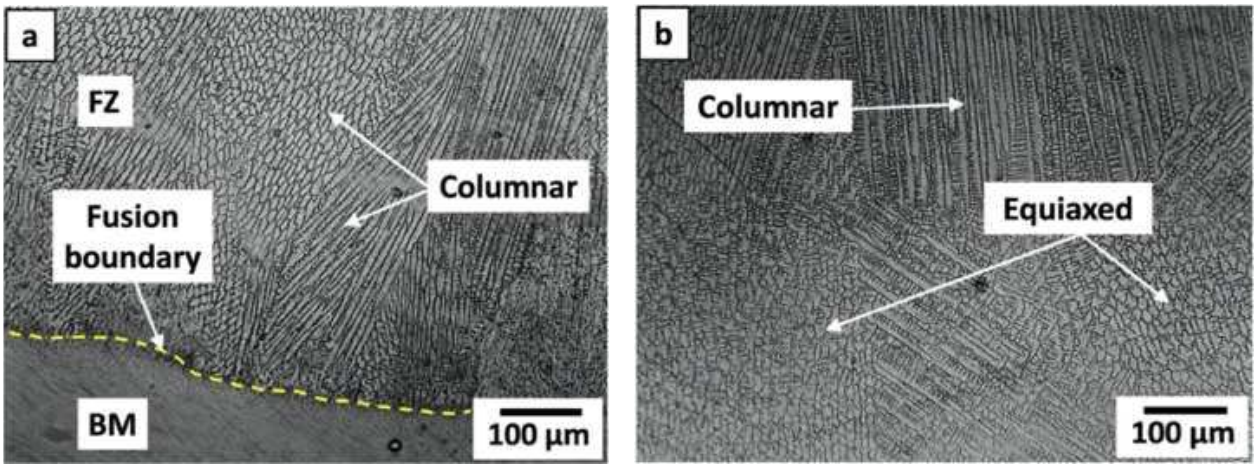

Fig. 4. FZ microstructure of 600 A and 0.2 s at (a) fusion boundary (b) centre of the weld

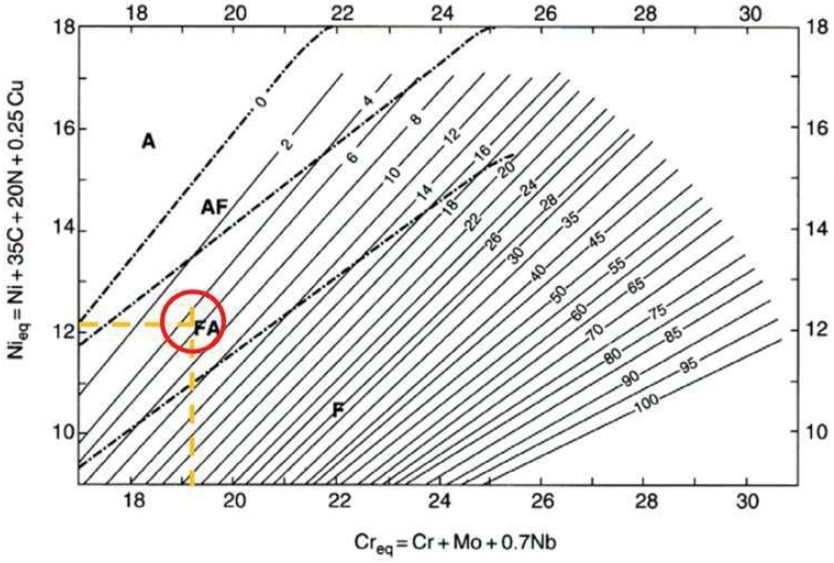

Fig. 5. WRC-1992 constitutional diagram. Adapted from [31]

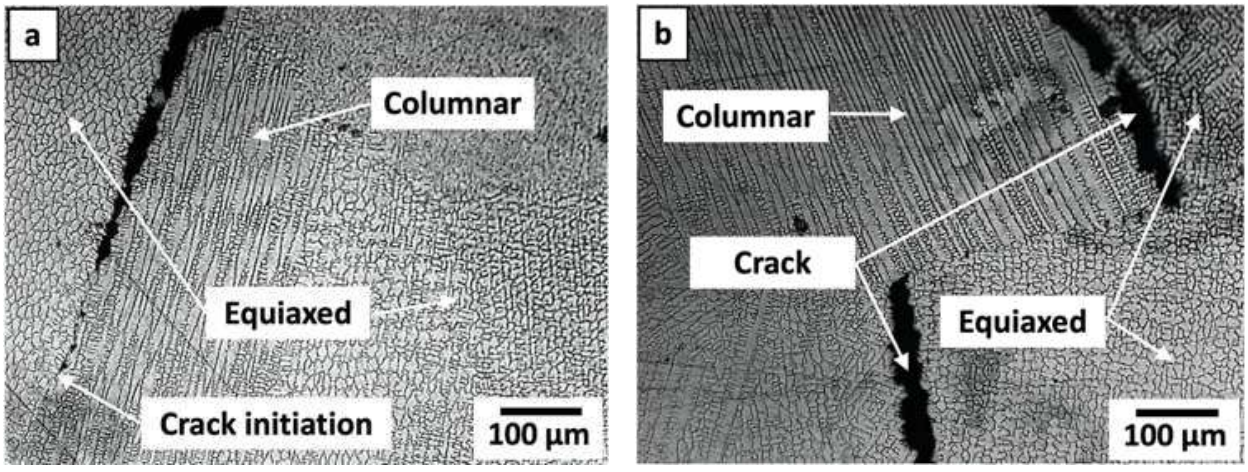

Fig. 6. FZ Solidification cracking at the FZ (a) crack initiation between columnar and equiaxed modes (b) cracks at centre of the weld at 600 A 0.2 s

3.2. Mechanical properties

Microhardness

Microhardness results, Figure 8, showed a reduction in the HAZ at the stud side. The loss in hardness in this region is strongly linked with the cold worked condition of the stud, which has a greater response to softening by welding thermal cycle than the annealed BM plate [32]. Generally, HAZ of 800 A welding joint recorded lower hardness than 400 A and 600 A, where the higher heat input has led to more grain growth [3]. In FZ, the peak hardness of 254 HV recorded with 800 A. While with 400 and 600 A, the hardness readings were 218 HV and 236 HV respectively. The high hardness with 800 A is related to the microstructure of FZ, Figure 7, that consists a high portion of second phase ferrite resulted from FA solidification mode due to the high heat input. The presence of ferrite considered as an embedment for dislocation motion during deformation and consequently raises the hardness property [33].

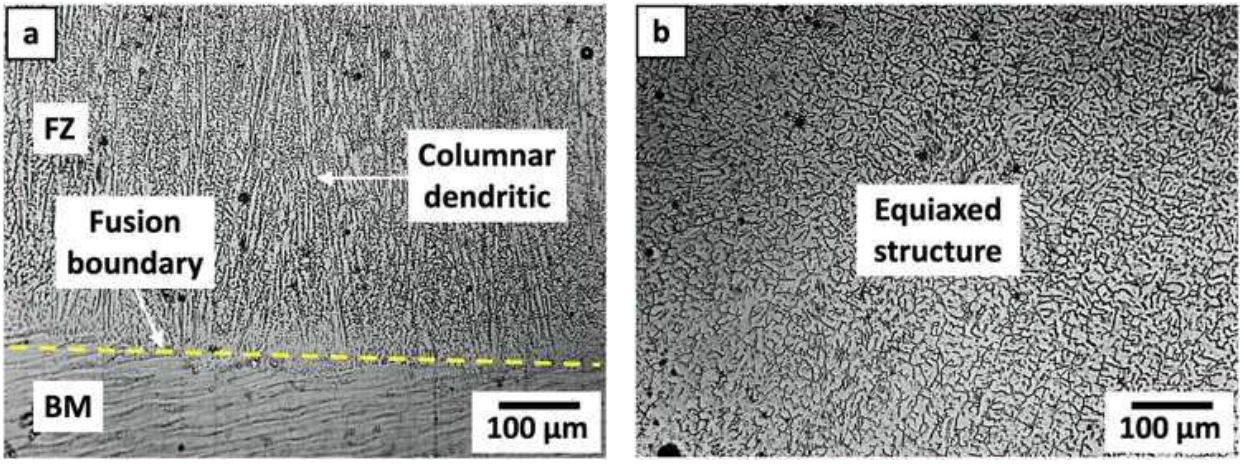

Fig. 7. FZ microstructure of 800A and 0.2 s at (a) fusion boundary (b) centre of the weld

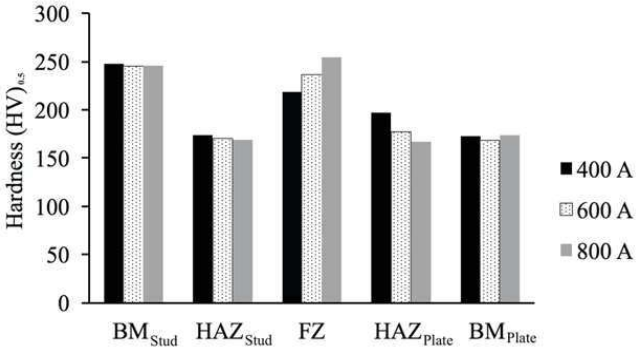

Fig. 8. HV numbers in different regions and welding currents at 0.2 s welding time

Torque strength

The impact of welding time on the torque strength for each welding current is presented in Figure 9. Each welding current had three samples. It was observed that heat input has a significant effect on the torsional strength. At 400 A welding current, the torque strength increases with increasing welding time. Short welding time produces low heat input for a particular current, which could be insufficient to melt both the stud and the BM therefore incomplete fusion may occur [2]. This can be combined with the formation of small weld reinforcement and small FZ around the stud in addition to the presence of voids as shown in Figure 10, which affects negatively on the torque strength of the weldment [34] . With increasing welding time, the torsional stress increases from 41 N.m at 0.2 s to 59 N.m at 0.4 s. However, this still lower than the minimum torsional stress (MTS) for 316L (which is 65 N.m according to ISO 3506-1, 2009) as shown in Figure 9. With increasing the welding current to 600 A, the torque strength slightly increased. Though, the relationship between torque strength and welding time has the same behaviour as 400 A. Since the torque strength increases with increasing welding time (Fig. 9). It can be clearly seen in Figure 11 that the 600 A is still insufficient at 0.2 s welding time where well-defined voids that resulted from low heat input were observed.

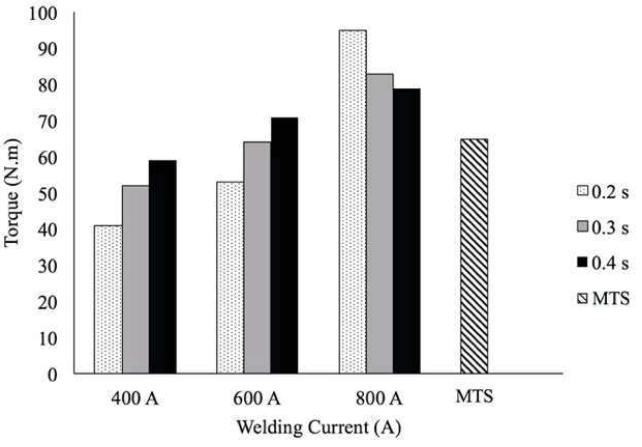

Fig. 9. Torque strength as a function of welding time for different welding currents. (MTS) is minimum breaking torsional stress for AISI 316L stainless steel

Interestingly, at 800 A welding current (Fig. 12), the torque strength recorded an increment at all welding times. This rise in torque strength was due to the effect of weld

microstructure, which contains the second phase ferrite in relatively high percentage (presence of FA solidification mode in 800A as shown in Fig. 7) that enhanced the torque resistance of the weldment. However, the relationship between torque strength and welding time showed an opposite behaviour where highest torsional strength resistance of 95 N.m was recorded at 0.2 s welding time then decreased to 79 N.m at 0.4 s. High welding current with long welding time might produce an excessive heat input [2] that led to reduce the diameter of the stud at the joint and produce weld undercut defect as can be seen in Figure 13. It is worth to mention that a good weld reinforcement combined with sound weld that is free of cracks and voids was obtained with 800 A and 0.2 s welding time as seen in Figure 12. Consequently, these welding conditions can be considered the optimum.

Fracture analysis

The mechanical performance of the joint was also evaluated by examining the failure behaviour of the welds after torque test. The examination was done under SEM at the fractured region (stud/plate interface). It was noticed that the fracture occurred in the HAZ of stud for all welding conditions. Figure 14 shows the failure mode with fine and uniform dimples confirming the ductile manner of failure under torsional force, that is in line with hardness results, which showed that HAZ is the softest region of welding joint.

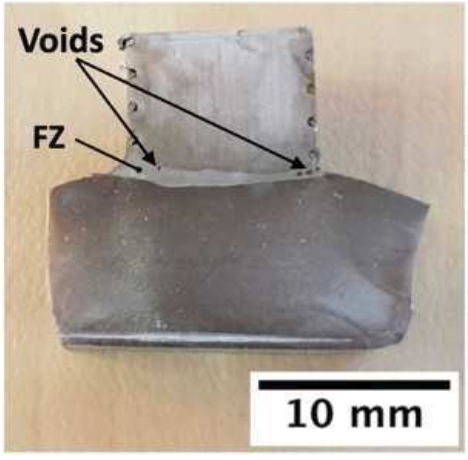

Fig. 10. Cross-section of 400 A, 0.2 s

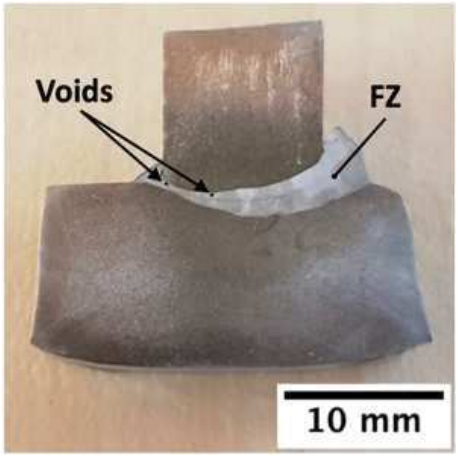

Fig. 11. Cross-section of 600 A, 0.2 s

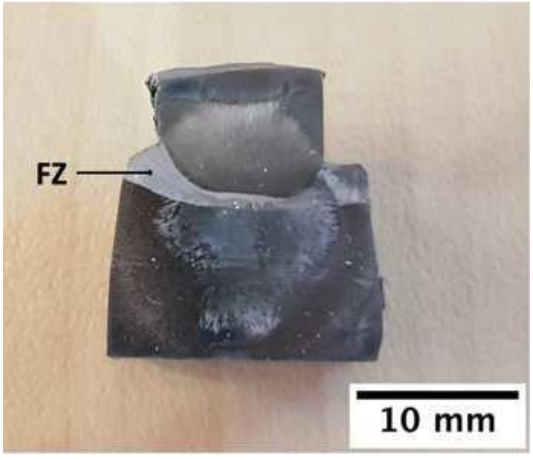

Fig. 12. Cross-section of 800 A, 0.2 s

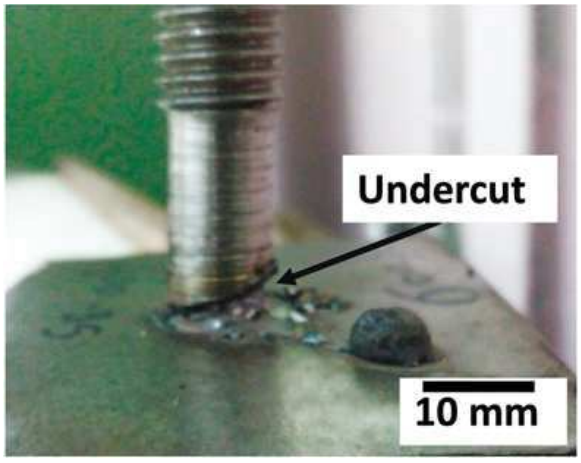

Fig. 13. Weld undercut defect of 800 A and 0.4 s

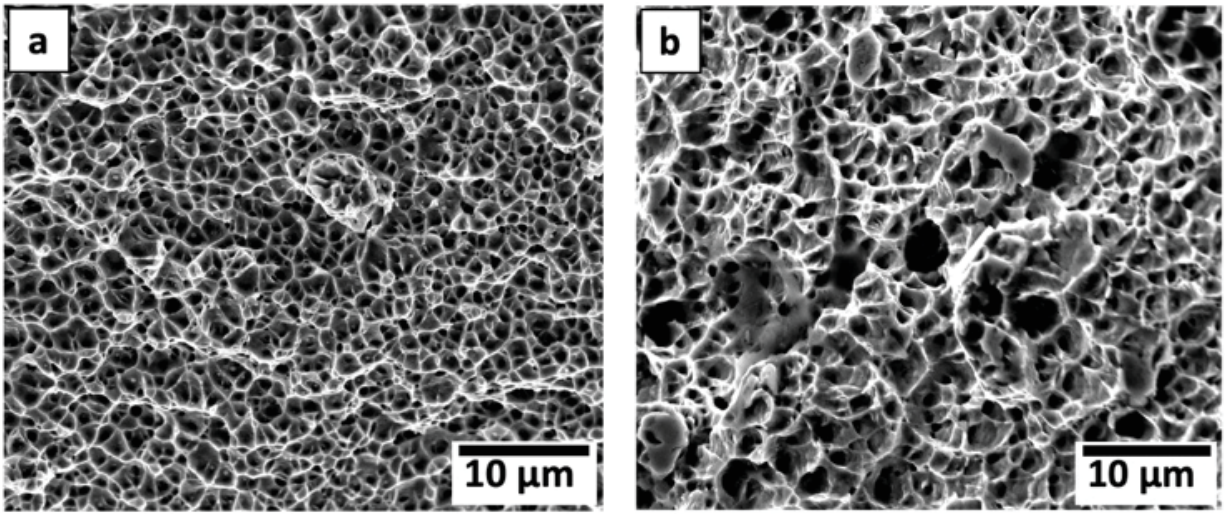

Fig. 14. SEM Fractography microstructure of fractured surface of (a) 600A, 0.2s and (b) 800A, 0.2s

4. Conclusions

- ASW of AISI 316L stainless steel studs to AISI 316L plate was successfully performed using a range of welding currents and times.
- FZ microstructure at 400 and 600A welding current with 0.2 s welding time characterized with type A solidification mode where a diffusionless transformation has occurred.
- At 800 A and 0.2 s, microstructure consisted of ferrite and austenite phases that resulted from FA solidification mode.
- Weld solidification cracking was detected in the fully austenitic microstructure. The cracks were mostly located along the solidification transition region called parting.
- Highest hardness and torque strength were recorded in FZ at 800 A and 0.2 s welding conditions due to the presence of ferrite phase.

References

[1] A.B. Başyiğit, A. Kurt, Investigation of the weld properties of dissimilar S32205 duplex stainless steel with AISI 304 steel joints produced by arc stud welding, Metals 7/3(2017) 77, DOI: https://doi.org/ 10.3390/ met7030077.

[2] N.F. Yilmaz, A.A. Hamza, Effect of Process Parameters on mechanical and microstructural properties of arc stud welds, Materials Testing 56/10 (2014) 806-811, DOI: https://doi.org/ 10.3139/120.110629.

[3] M. Alali, I. Todd, B. Wynne, Through-thickness microstructure and mechanical properties of electron beam welded 20 mm thick AISI 316L austenitic stainless steel, Materials & Design 130 (2017) 488-500, DOI: https://doi.org/ 10.1016/j.matdes.2017.05.080.

[4] A. Balitsky, I. Kostyuk, O. Krokhmalny, Psysical-mechanical non-homogeneity of welded joints of high-nitrogen Cr-Mn steels and their corrosion resistance, Paton Welding Journal C/C of Avtomaticheskaia Svarka 2003/2 (2003) 26-29.

[5] H. Soltanzadeh, J. Hildebrand, M. Kraus, M. Asadi, Modelling of a stud arc welding joint for temperature field, Microstructure Evolution and residual stress, Proceedings of the Pressure Vessels and Piping Conference "ASME 2016", American Society of Mechanical Engineers, 2016, V06BT06A002.

[6] H.A. Chambers, Principles and practices of stud welding, PCI Journal 46/5 (2001) 46-58, DOI: https://doi.org/10.15554/pcij.09012001.46.58.

[7] E.N. Abbas, S. Omran, M. Alali, M.H. Abass, A.N. Abood, Dissimilar Welding of AISI 309 Stainless Steel to AISI 1020 Carbon Steel Using Arc Stud Welding, Proceedings of the 2018 International Conference on Advanced Science and Engineering "ICOASE", 2018, 462-467.

[8] R. Unnikrishnan, K.S.N. Satish Idury, T.P. Ismail, A. Bhadauria, S.K. Shekhawat, R.K. Khatirkar, S.G.

Sapate, Effect of heat input on the microstructure, residual stresses and corrosion resistance of 304L austenitic stainless steel weldments, Materials Characterization 93 (2014) 10-23, DOI: https://doi.org/ 10.1016/ j.matchar.2014.03.013.

[9] N. Moslemi, N .Redzuan, N. Ahmad, T.N. Hor, Effect of current on characteristic for 316 stainless steel welded joint including microstructure and mechanical properties," Procedia CIRP 26 (2015) 560-564, DOI: https://doi.org/10.1016/j.procir.2015.01.010.

[10] J. Yan, M. Gao, X. Zeng, Study on microstructure and mechanical properties of 304 stainless steel joints by TIG, laser and laser-TIG hybrid welding, Optics and Lasers in Engineering 48/4 (2010) 512-517, DOI: https://doi.org/10.1016/j.optlaseng.2009.08.009.

[11] T. Tabish, T. Abbas, M. Farhan, S. Atiq, T. Butt, Effect of heat input on microstructure and mechanical properties of the TIG welded joints of AISI 304 stainless steel, International Journal of Scientific & Engineering Research 5/7 (2014) 1532-1541.

[12] E. Zumelzu, J. Sepulveda, M. Ibarra, Influence of microstructure on the mechanical behaviour of welded 316 L SS joints, Journal of Materials Processing Technology 94/1 (1999) 36-40, DOI: https://doi.org/ 10.1016/S0924-0136(98)00450-6.

[13] S. Tjong, S. Zhu, N. Ho, J. Ku, Microstructural characteristics and creep rupture behavior of electron beam and laser welded AISI 316L stainless steel, Journal of Nuclear Materials 227/1-2 (1995) 24-31, DOI: https://doi.org/10.1016/0022-3115(95)00142-5.

[14] B. Joseph, D. Katherasan, P. Sathiya, C.S. Murthy, Weld metal characterization of 316L (N) austenitic stainless steel by electron beam welding process, International Journal of Engineering, Science and Technology 4/2 (2012) 169-176.

[15] J. Lippold, Centerline cracking in deep penetration electron beam welds in Type 304L stainless steel, Welding Journal 64/5 (1985) 127s-136s.

[16] A.A. Shehab, S.K. Sadrnezhaad, M.J. Torkamany, M. Fakouri Hasanabadi, M. Alali, A.K. Mahmoud, M.H. Abass, A.H. Kokabi, Ring-like laser spot welding of Ti grade2 to AAl3105-O using AlSiMg filler metal, Optik (2019) 163630, DOI: https://doi.org/ 10.1016/ j.ijleo.2019.163630.

[17] O. Balyts'kyi, I. Kostyuk, Strength of welded joints of Cr–Mn steels with elevated content of nitrogen in hydrogen-containing media, Materials Science 45/1 (2009) 97-107, DOI: https://doi.org/10.1007/s11003-009-9166-7.

[18] H.M. Mahan, Effect of Heat Treatments on the Mechanical Properties of Welded Joints of Alloy Steel by Arc Welding, Diyala Journal of Engineering Sciences 12/2 (2019) 44-53, DOI: https://doi.org/ 10.26367/ DJES/VOL.12/NO.2/4.

[19] J. Kell, J. Tyrer, R. Higginson, R. Thomson, Microstructural characterization of autogenous laser welds on 316L stainless steel using EBSD and EDS, Journal of Microscopy 217/2 (2005) 167-173, DOI: https://doi.org/10.1111/j.1365-2818.2005.01447.x.

[20] T. Siewert, C. McCowan, D. Olson, Ferrite number prediction to 100 FN in stainless steel weld metal, Welding Journal 67/12 (1988) 289s-298s.

[21] A. Choubey, V. Jatti, Influence of heat input on mechanical properties and microstructure of austenitic 202 grade stainless steel weldments, WSEAS Transactions on Applied and Theoretical Mechanics 9 (2014) 222-228.

[22] S. Semiatin, G. Lahoti, J. Jonas, ASM metals handbook, ASM, Metals Park, OH, 1985.

[23] D. Kotecki, J. Lippold, Welding metallurgy and weldability of stainless steels, Wiley ,Hoboken, NJ, 2005; B. Barbero, E. Ureta Comparative study of different digitization techniques and their accuracy, Computer-Aided Design 43/1 (2011) 188-206, DOI: https://doi.org/10.1016/j.cad.2010.11.005.

[24] S. Celen, S. Karadeniz, H. Özden, Effect of laser welding parameters on fusion zone morphological, mechanical and microstructural characteristics of AISI 304 stainless steel, Materialwissenschaft und Werkstofftechnik 39/11 (2008) 845-850, DOI: https://doi.org/10.1002/mawe.200800384.

[25] M. Perricone, J. Dupont, T. Anderson, C. Robino, J. Michael, An investigation of the massive transformation from ferrite to austenite in laser-welded mo-bearing stainless steels, Metallurgical and Materials Transactions A 42/3 (2011) 700-716, DOI: https://doi.org/10.1007/s11661-010-0433-x.

[26] S. Baghjari, S. AkbariMousavi, Experimental investigation on dissimilar pulsed Nd: YAG laser welding of AISI 420 stainless steel to kovar alloy, Materials & Design 57 (2014) 128-134, DOI: https://doi.org/10.1016/ j.matdes.2013.12.050.

[27] V. Shankar, T. Gill, S. Mannan, S. Sundaresan, Solidification cracking in austenitic stainless steel welds, Sadhana 28/3-4 (2003) 359-382, DOI: https://doi.org/10.1007/ BF02706438.

[28] J. Yu, M. Rombouts, G. Maes, Cracking behavior and mechanical properties of austenitic stainless steel parts

produced by laser metal deposition, Materials & Design 45 (2013) 228-235, DOI: https://doi.org/10.1016/j.matdes. 2012.08.078.
[29] J .Elmer, S. Allen, T. Eagar, Microstructural development during solidification of stainless steel alloys, Metallurgical Transactions A 20/10 (1989) 2117-2131, DOI: https://doi.org/10.1007/ BF02650298.
[30] J. Sule, S. Ganguly, H. Coules, T. Pirling, Application of local mechanical tensioning and laser processing to refine microstructure and modify residual stress state of a multi-pass 304L austenitic steels welds, Journal of Manufacturing Processes 18 (2015) 141-150, DOI: https://doi.org/10.1016/j.jmapro.2015.03.003.
[31] D. Kotecki, T. Siewert, WRC-1992 constitution diagram for stainless steel weld metals: a modification of the WRC-1988 diagram, Welding Journal 71/5 (1992) 171s-178s.
[32] S. Kou, Welding metallurgy, John Wiley & Sons, 2003.
[33] D.R. Askeland, P. Webster, The science and engineering of materials, Springer, 1996.
[34] Š. Klarić, I. Kladarić, D. Kozak, A. Stoić, Ž. Ivandić, I. Samardžić, The influence of the stud arc welding process parameters on the weld penetration, Scientific Bulletin Series C: Fascicle Mechanics, Tribology, Machine Manufacturing Technology 23 (2009) 79-84.